



HAL
open science

Investigating the action of the microalgal pigment marennine on *Vibrio splendidus* by in vivo ²H and ³¹P solid-state NMR

Zeineb Bouhleb, Alexandre A Arnold, Jean-Sébastien Deschênes, Jean-Luc Mouget, Dror E Warschawski, Réjean Tremblay, Isabelle Marcotte

► To cite this version:

Zeineb Bouhleb, Alexandre A Arnold, Jean-Sébastien Deschênes, Jean-Luc Mouget, Dror E Warschawski, et al.. Investigating the action of the microalgal pigment marennine on *Vibrio splendidus* by in vivo ²H and ³¹P solid-state NMR. *Biochimica et Biophysica Acta: Biomembranes*, 2021, 1863 (9), pp.183642. 10.1016/j.bbamem.2021.183642 . hal-03242868

HAL Id: hal-03242868

<https://hal.science/hal-03242868>

Submitted on 7 Jun 2021

HAL is a multi-disciplinary open access archive for the deposit and dissemination of scientific research documents, whether they are published or not. The documents may come from teaching and research institutions in France or abroad, or from public or private research centers.

L'archive ouverte pluridisciplinaire **HAL**, est destinée au dépôt et à la diffusion de documents scientifiques de niveau recherche, publiés ou non, émanant des établissements d'enseignement et de recherche français ou étrangers, des laboratoires publics ou privés.

1 **Investigating the action of the microalgal pigment marennine on *Vibrio***
2 ***splendidus* by *in vivo* ²H and ³¹P solid-state NMR**

3 *Zeineb Bouhlef*^{1,2}, *Alexandre A. Arnold*², *Jean-Sébastien Deschênes*³ *Jean-Luc Mouget*⁴, *Dror E.*
4 *Warschawski*^{2,5}, *Réjean Tremblay*¹ and *Isabelle Marcotte*^{2*}

5

6 ¹ Institut des Sciences de la Mer de Rimouski, Université du Québec à Rimouski, G5L 3A1,
7 Rimouski, Canada

8

9 ² Department of Chemistry, Université du Québec à Montréal, P.O. Box 8888, Downtown
10 Station, H3C 3P8, Montreal, Canada

11

12 ³ Mathematics, computer science and engineering department, Université du Québec à Rimouski,
13 G5L 3A1, Rimouski, Canada.

14

15 ⁴ Mer-Molécules-Santé, MMS, FR CNRS 3473, IUML, Le Mans Université, 72000 Le Mans,
16 France

17

18 ⁵ Laboratoire des Biomolécules, LBM, CNRS UMR 7203, Sorbonne Université, École normale
19 supérieure, PSL University, 75005 Paris, France

20

21 *Corresponding author

22 Tel: 1-514-987-3000 #5015

23 Fax: 1-514-987-4054

24 E-mail: marcotte.isabelle@uqam.ca

25

26

27 **ABSTRACT**

28 This work investigates the potential probiotic effect of marennine - a natural pigment produced
29 by the diatom *Haslea ostrearia* - on *Vibrio splendidus*. These marine bacteria are often
30 considered a threat for aquaculture, therefore chemical antibiotics can be required to reduce
31 bacterial outbreaks. *In vivo* ^2H solid-state NMR was used to probe the effects of marennine on the
32 bacterial membrane in the exponential and stationary phases. Comparisons were made with
33 polymyxin B (PxB) - an antibiotic used in aquaculture and known to interact with Gram(-)
34 bacteria membranes. We also investigated the effect of marennine using ^{31}P solid-state NMR on
35 model membranes. Our results show that marennine has little effect on phospholipid headgroups
36 dynamics, but reduces the acyl chain fluidity. Our data suggest that **the two antimicrobial agents**
37 **perturb *V. splendidus* membranes through different mechanisms.** While PxB would alter the
38 bacterial outer and inner membranes, marennine would act through a membrane stiffening
39 mechanism, without affecting the bilayer integrity. Our study proposes this microalgal pigment,
40 which is harmless for humans, as a potential treatment against vibriosis.

41 **KEYWORDS**

42 Antimicrobial pigment, polymyxin B, membrane fluidity, model membranes, ^{31}P and ^2H NMR,
43 in-cell NMR.

44 **ABBREVIATIONS**

45 ASW, artificial sea water; Chloroform-D, deuterated chloroform; CL, cardiolipin; CSA, chemical
46 shift anisotropy; D_2O , deuterium oxide; PA- d_{31} , deuterated palmitic acid; DOPE,
47 dioleoylphosphatidylethanolamine; LB, Lysogeny broth; LPS, lipopolysaccharides; M_2 , second
48 spectral moment; MAS, magic angle spinning; MIC, minimum inhibitory concentration; MLV,
49 multilamellar vesicle; MTT, 3-(4,5-dimethylthiazol-2-yl)-2,5-diphenyltetrazolium bromide; OA,
50 oleic acid; OD, optical density; PE, phosphatidylethanolamine; PG, phosphatidylglycerol; POPE,
51 1-palmitoyl-2-oleoyl-sn-glycero-3-phosphoethanolamine; POPG, 1-palmitoyl-2-oleoyl-sn-
52 glycero-3-phospho-(1'-rac- glycerol); **PSU, Practical Salinity Unit**; PxB, polymyxin B; SSB,
53 spinning side band; SS-NMR, solid-state nuclear magnetic resonance.

54 INTRODUCTION

55 According to the World Bank, aquaculture is a growing industry and a promising alternative to
56 the fishery crisis [1]. However, like many commercial activities, aquaculture relies on intensive
57 production and in the context of global warming, the stress that cultured animals may undergo
58 can lead to diseases and losses [2,3]. Vibriosis - an infection caused by *Vibrio* bacteria - is
59 amongst the most problematic pathologies in the world for aquatic species [4]. *Vibrio* outbreaks
60 are often associated with important mortality and *Vibrio splendidus* are almost exclusive to
61 bivalve infection especially during the first stages of culture [5,6].

62 For years, aquaculture has counted on antimicrobial agents for prophylactic or therapeutic
63 purposes, and too extensively in some cases such as shrimp and salmon farming [7-9].
64 Nowadays, regulations in aquaculture are stricter since bacterial resistance is a considerable issue
65 [8,10]. Consequently, there is a growing need to develop novel therapeutic approaches that are
66 more environmentally friendly and less harmful for food human consumption than conventional
67 synthetic antibiotics. New strategies include brood-stock conditioning [7], as well as the use of
68 natural biologically active alternatives such as immuno-stimulants, bacteriophages and probiotics
69 [11,12].

70 Marennine is a natural blue pigment and a promising therapeutic alternative against vibriosis
71 in aquaculture [13,14]. It is secreted by *Haslea ostrearia*, a marine microalga responsible for the
72 noticeable greening of oysters cultured in the French Marennes region and harmless for the
73 consumers. Recent works showed that marennine is a water-soluble 10 kDa polyphenol with
74 possibly a glycosidic skeleton, however, the exact structure and nature of this molecule is today
75 still unknown [15]. The probiotic potential of marennine against aquatic Gram(-) bacteria
76 including *Vibrio* species, has already been demonstrated [16-18]. Turcotte *et al.* also showed that
77 in the presence of marennine extracts, the pathogenicity of Gram(-) *V. splendidus* was suppressed
78 [14]. However, the action mechanism of marennine towards marine bacteria has not yet been
79 elucidated. Considering the high molecular weight of marennine and its unlikely penetration in
80 the bacterial membrane, the pigment would favor an interaction with the outer-membrane of
81 Gram(-) bacteria, as suggested by a solid-state nuclear magnetic resonance (SS-NMR) study on
82 *Escherichia coli* [19].

83 The objective of this work was to investigate the action mechanism of marennine towards the
84 marine bacterium *V. splendidus*, more specifically the indigenous environmental strain (7SHRW)
85 isolated from the St. Lawrence estuary, which causes significant mortality of blue mussel and
86 scallops' larvae. Marennine has previously been shown to inhibit the virulent action of this strain
87 [14]. To do so, we studied the interaction of marennine with 7SHRW using *in vivo* ^2H SS-NMR,
88 and with model membranes using ^{31}P SS-NMR. Deuterium SS-NMR provides valuable
89 information on acyl chain dynamics and organization in membrane systems made of deuterated
90 phospholipids, while phosphorous NMR is a valuable tool to probe lipid headgroup
91 perturbations. Traditionally used to study model membranes, the deuterium labelling of
92 membrane lipids in intact bacteria enabled *in vivo* ^2H SS-NMR experiments on *E. coli*, *Bacillus*
93 *subtilis*, and more recently *V. splendidus* [19-22]. It is also a useful tool to examine membrane
94 interactions with exogenous molecules such as detergents, drugs, and peptides, at a molecular-
95 level [23].

96 In this work, the effect of marennine on *V. splendidus* membranes at two different growth
97 stages (mid-log and stationary phase) is compared to a commercial antibiotic, polymyxin B
98 (PxB), which has a well-documented action mechanism. Polymyxins are amongst the most
99 commonly used antibiotics in aquaculture and are known to specifically act against Gram(-)
100 bacteria by damaging their membranes [24-26]. However, recent regulations have prohibited the
101 use of PxB in aquaculture [24]. By comparing the interaction of marennine and PxB with *V.*
102 *splendidus* membranes, we propose a possible mechanism involved in the bactericidal action of
103 marennine, and the use of this natural pigment as an alternative to synthetic antibiotics.

104

105 **MATERIALS AND METHODS**

106 ***Materials***

107 Oleic acid (OA) and deuterated palmitic acid (PA- d_{31}), as well as deuterium depleted water, 3-
108 (4,5-dimethylthiazol-2-yl)-2,5-diphenyltetrazolium bromide (MTT), and PxB sulfate salt, were
109 all purchased from Sigma Aldrich (Oakville, ON, Canada). Synthetic lipids 1-palmitoyl-2-oleoyl-
110 sn-glycero-3-phosphoethanolamine (POPE), 1-palmitoyl-2-oleoyl-sn-glycero-3-phospho-(1'-rac-
111 glycerol) (POPG), and cardiolipin (CL) were purchased from Avanti Polar Lipids (Alabaster, AL,

112 USA). Tween-20 (polyethylene glycol sorbitan monolaurate) and tris(hydroxymethyl)-
113 aminomethane were acquired from BioShop (Burlington, ON, Canada), while LB Broth Miller
114 was obtained from BioBasic (Markham ON, Canada), and ethylenediaminetetraacetic acid
115 (EDTA) from Fisher Scientific (Fair Lawn, NJ, USA). Deuterium oxide (D₂O) and deuterated
116 chloroform (chloroform-D) were respectively bought from CDN Isotopes (Pointe-Claire, Quebec,
117 Canada) and Cambridge Isotope Laboratories (Endover, MA, USA). The solution of marennine
118 tested was produced by *H. ostrearia* strain NCC-136-isolated from Bourgneuf Bay, France.
119 Microalgae were cultured with the use of fluorescent growth-light at an intensity corresponding
120 to a photon flux of 180 $\mu\text{mol photons}\cdot\text{m}^{-2}\cdot\text{s}^{-1}$ and 14/10 hours light/dark cycle in filtered seawater
121 with a salinity of 28 PSU, at 20°C [14]. The supernatant was then extracted and purified
122 according to previously published methods [13].

123 ***Bacterial growth and ²H labelling***

124 *V. splendidus* 7SHRW [27] were grown in LB medium and deuterated using equal proportions
125 of OA and PA-d₃₁ (0.3 mM each) micellized in 0.14 mM of Tween-20 detergent to insure fatty
126 acid intake, as described in Bouhleb *et al.* [22]. The growth kinetics was monitored with a
127 multiple plate reader (Infinite M200 TECAN, Männedorf, Switzerland) using 24-well plates, by
128 measuring absorbance at 600 nm every 30 min. Typically, 3 to 4 wells were used for each
129 treatment. Bacteria were harvested at two different moments, *i.e.*, after the mid-log phase and at
130 the early-stationary phase, centrifuged (2600 g, 10 min), then pellets were washed twice with a
131 sterile NaCl solution (154 mM) prepared with nanopure water. A standard curve relating optical
132 density of the culture and the corresponding dry weight was determined after pellet
133 lyophilization.

134 ***Antimicrobial activity measurement***

135 The antimicrobial activity of marennine and PxB towards *V. splendidus* was assessed by
136 measuring the minimum inhibitory concentration (MIC) using a serial dilution technique [17,28].
137 An LB medium (171 mM NaCl) was used for all dilutions, and final concentrations ranged from
138 1.25 to 400 $\mu\text{g}/\text{mL}$ for marennine, and from 1 to 32 $\mu\text{g}/\text{mL}$ for PxB. A total of 200 μL of initial
139 cell suspension was transferred into a 100-well plate to monitor the growth kinetics with a
140 multiple-plate reader at 25°C. The absorbance at 600 nm was recorded every 30 min over a 48h

141 period. The absorbances were ~0.5 in the mid-log phase and ~0.8 in the stationary phase as
142 shown in the growth curves (Figures S1 and S2).

143
144

145 **Bacteria exposure for NMR experiments**

146 Marennine and PxB assays were performed at selected concentrations in triplicate on ²H-
147 labelled bacteria, adjusted to correspond to approximately 10 ± 2 mg (dry weight).

148 For PxB exposures, ²H-labelled bacteria pellets were resuspended in a 1 mL solution of NaCl
149 (154 mM) in ²H-depleted water, with the appropriate amount of antibiotics (final concentration of
150 1 µg/mL and the MIC), and vortexed before a 10 min incubation. For marennine experiments,
151 ²H-labelled bacteria pellets were resuspended in a 50 mL solution of ²H-depleted artificial
152 seawater (ASW) containing NaCl (480 mM), MgSO₄ (28 mM), MgCl₂ (24 mM), CaCl₂ (16 mM)
153 and NaHCO₃ (2.4 mM), with a pH adjusted to 8.0 ± 0.1, with the appropriate amount of
154 marennine (final concentration of 2 µg/mL and at the MIC). Exposures were carried out in 250
155 mL Erlenmeyer flasks placed on a rotary shaker (100 rpm) at a temperature of 22 ± 1 °C for 2h.
156 Note that nutrients were purposely discarded during marennine exposure to avoid continuing
157 bacterial growth, and concomitant changes in membrane fluidity as previously reported [22]. The
158 lack of nutrients and 2h shaking in ASW have a little effect on cell viability (90% ± 5), as
159 estimated with an MTT 3-(4,5-dimethylthiazol-2-yl)-2,5-diphenyltetrazolium bromide) test [20].
160 Bacteria exposed to ASW only are considered as a control. Both types of sample pellets (control
161 and exposed to marennine) came from the same culture replicates.

162 Bacteria were collected immediately after exposure to PxB or marennine, and centrifuged at
163 3200 g for 5 min. Pellets were then washed in a solution of 9‰ NaCl in ²H-depleted water, then
164 centrifuged at 3200 g again for 5 min. The final pellet was used to fill a 4-mm zirconium oxide
165 rotor, which corresponds to approximately 90 mg of hydrated bacteria.

166 **Phospholipid analysis of *V. splendidus***

167 Bacteria harvested at the early stationary phase were washed with NaCl solution (154 mM) and
168 freeze-dried. Lipids were analyzed following the protocol of Mahabadi *et al.* (to be submitted). In
169 short, lipids were extracted according to the protocol of Folch [29] using
170 dichloromethane/methanol (2:1 CH₂Cl₂/MeOH v/v) and 0.88% KCl solution in a Potter glass

171 homogenizer. Polar lipids were separated from neutral lipids by elution through a silica gel
172 column (30×5 mm) hydrated to 6% with distilled water [30]. Final polar lipid extracts were
173 dissolved in a mixture composed of 500 µL of deuterated chloroform, 200 µL methanol, 50 µL of
174 an aqueous EDTA (200 mM) solution at pH 6, vortexed, transferred to a solution NMR glass tube
175 for ³¹P NMR analysis, and stabilized until a biphasic solution was obtained.

176 ***Preparation of model bacterial membranes***

177 Model membranes were prepared from lipid mixtures of POPE, POPG and CL in proportions
178 similar to *V. splendidus* membrane composition, deduced from the ³¹P solution NMR experiments
179 (85% phosphatidylethanolamine (PE), 10% phosphatidylglycerol (PG) and 5% cardiolipin (CL)
180 (in mole %)). For each sample, 30 mg of phospholipid powder mixture was dissolved in
181 CH₂Cl₂/MeOH (3:1) and dried under a stream of N₂ gas for 30 min. Remaining organic residues
182 were further evaporated overnight under vacuum. The dry lipid films were hydrated in 120 µL
183 buffer solution (Tris (100 mM), NaCl (100 mM), EDTA (2 mM) and D₂O; pH=8), resulting in
184 multilamellar vesicles (MLVs) which will be referred to as liposomes. For marennine-containing
185 samples, the appropriate pigment amount was dissolved in the buffer solution before lipid
186 hydration. All preparations were mechanically homogenized and processed through five cycles of
187 liquid N₂ freezing and thawing in a 35°C water bath. The MLV samples were subsequently filled
188 in 4 mm rotors for ³¹P SS- NMR analysis.

189 ***²H solid-state NMR experiments***

190 All ²H SS-NMR experiments were carried out using a Bruker Avance III HD Wide Bore 600
191 MHz NMR spectrometer (Milton, Ontario, Canada) and a double-resonance magic angle spinning
192 (MAS) probe tuned to 92.1 MHz. Samples were spun at 10 kHz and at 25°C. Since MAS
193 refocuses the ²H quadrupolar interaction, instead of the classic solid echo used in the static case,
194 the spectra were acquired using a Hahn Echo pulse sequence with 4 µs 90° pulses separated by an
195 echo delay of 96 µs, a recycle time of 0.5 s, 4096 scans, 32k points and a spectral width of 500
196 kHz, for a total of 43 min of acquisition time. Spectra were zero-filled to 64k points, and treated
197 with an exponential line broadening of 40 and 100 Hz for PxB and marennine sample spectra,
198 respectively.

199 Spectral moment analysis was performed using MestRenova software V6.0 (Mestrelab
200 Research, Santiago de Compostela, Spain) and a macro developed by Pierre Audet (Université

201 Laval, Québec, Canada). The second moment (M_2) was calculated using the following equation
202 [21]:

$$M_2 = \omega_r^2 \frac{\sum_{N=0}^{\infty} N^2 A_N}{\sum_{N=0}^{\infty} A_N}$$

203
204 where ω_r is the angular spinning frequency, N the side band number, and A_N the area of each
205 sideband obtained by spectral integration. The integration of the central peak includes the
206 residual HDO peak which leads to a systematic underestimation of the M2 by a maximum of
207 15%.

208 ***³¹P solid-state NMR experiments***

209 All ³¹P SS-NMR experiments were carried out using a Bruker Avance III HD Wide Bore 400
210 MHz NMR spectrometer (Milton, Ontario, Canada) operating at frequencies of 161.9MHz and
211 400.02 MHz for ³¹P and ¹H, respectively. Samples were analyzed at 25°C, 50°C and 75°C, with a
212 25 min equilibration step before each temperature. Temperatures were controlled to within ±
213 0.5°C, and chemical shifts were referenced relative to external H₃PO₄ set to 0 ppm. Static spectra
214 were recorded through a ¹H-decoupled Hahn echo pulse sequence with a ³¹P 90° pulse length of
215 3µs, a recycle delay of 3s, and 512 scans, in approximately 25 min.

216 Line shapes were fitted using the Bruker SOLA software. Vesicles shapes (spherical vs.
217 ellipsoidal) were determined using dedicated MATLAB scripts based on the analytical model of
218 Dubinnyi *et al.* [31], where the vesicle is described by the ratio ρ between the long and short axis
219 of the ellipsoid ($\rho=1$ if vesicles are spherical).

220 ***³¹P solution-state NMR experiments***

221 All ³¹P solution NMR experiments were performed at 25°C using a Bruker Avance III HD 600
222 MHz NMR spectrometer (Milton, Ontario, Canada) operating at frequencies of 242.84 MHz and
223 599.95 MHz for ³¹P and ¹H, respectively. For quantitative results, ³¹P spectra were recorded with
224 a 10 s recycle delay, continuous ¹H decoupling during acquisition, without NOE enhancement,
225 with 128 scans in approximately 22 min. Spectra were processed with an exponential line
226 broadening of 2 Hz.

227

228 **RESULTS AND DISCUSSION**

229 ***Minimum inhibitory concentration***

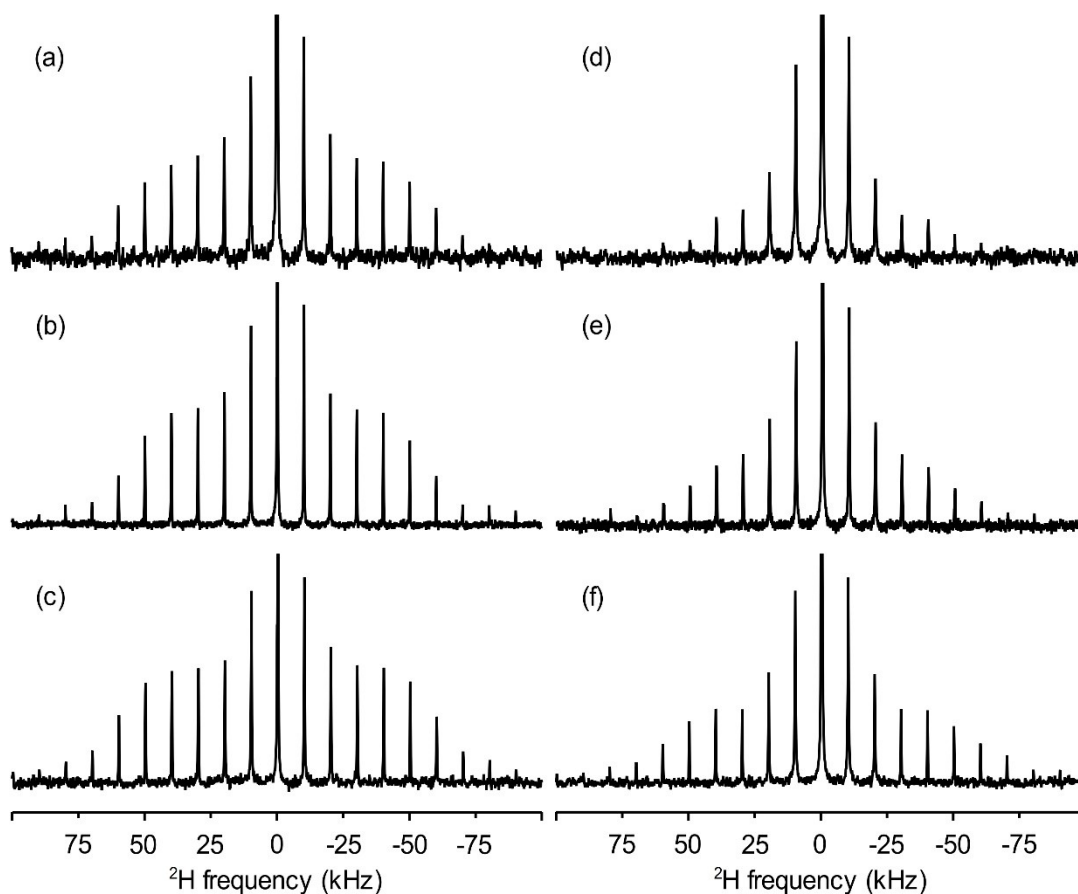
230 To quantify the antibacterial activity of marennine and PxB on *V. splendidus*, we determined
231 their minimum inhibitory concentration (MIC). The growth curves are displayed in the
232 Supplementary information section (Fig. S1 and S2). Values of 200 µg/mL and 8 µg/mL were
233 found for marennine and PxB, respectively. So far, marennine has been characterized as a
234 potential polyphenol with a glycosidic structure [13,15][13, 15], and its MIC is in the same range
235 as other plant polyphenol extracts acting on Gram(-) bacteria, *i.e.*, from 70 to 500 µg/mL on
236 *Vibrio* species [32,33][32, 33]. As for PxB, its MIC has been reported to range between 1 to 8
237 µg/mL depending on the bacterial species [34]. Here, we observe that the MIC of PxB for *V.*
238 *splendidus* is 8 times higher than that reported for *E. coli* [19]. We also notice a different
239 response of *V. splendidus* to marennine as compared to *E. coli*. Indeed, Tardy-Laporte *et al.*
240 reported a change in membrane fluidity when *E. coli* was exposed to 2 µg/mL of marennine in
241 NaCl (171 mM) solution for 15 min [19], while a longer exposure time (2h) was required to
242 observe this effect for *V. splendidus* at the same marennine concentration [19]. However, *V.*
243 *splendidus* showed membrane collapse after 2 hours of exposure in NaCl (171 mM) solution. We
244 have thus used artificial seawater (ASW) in this work since membrane integrity is preserved for
245 up to 12 hours in ASW (data not shown), and to eliminate any possible effect of the salt and
246 better focus on the antibacterial activity.-

247 ***Effect of marennine and polymyxin B on V. splendidus membranes***

248 To better understand the action of marennine and PxB on *V. splendidus*, their effect was
249 studied by ²H SS-NMR at the MIC but also at a lower concentration, during the exponential and
250 stationary phases. In practice, concentrations below the MIC are typically used in aquaculture [8].
251 As demonstrated in a previous work, membrane lipid chains in *V. splendidus* can be ²H-labelled
252 by growing marine bacteria in a medium enriched with PA-d₃₁ [22]. The presence of OA ensures
253 a lipid profile closer to unlabelled bacteria. A labelling percentage of 69% and 55% of total
254 palmitic acid can be reached in the exponential and in the stationary phases, respectively. The
255 second spectral moment (M₂) was used to quantify the membrane lipid acyl chain ordering. The
256 greater the M₂, the higher the lipid chain ordering. As shown by Warnet *et al.*, combination of

257 MAS and ^2H SS-NMR provides a fast method to ensure the *in vivo* characterization of bacteria
258 [21]. *In vivo* conditions were confirmed for *V. splendidus* by estimating the bacterial viability
259 using an MTT reduction assay [21] after 2 h of MAS experiments, which was $95 \pm 5 \%$.

260 Figure 1 shows the effect of marennine on *V. splendidus* at low concentration (2 $\mu\text{g}/\text{mL}$) and
261 at the MIC (200 $\mu\text{g}/\text{mL}$), with corresponding M_2 values presented in Table 1. The “low”
262 marennine concentration employed here is 20 times that reported to be effective on *V. splendidus*
263 (7SHRW) in aquaculture conditions [14]. Spectral analysis reveals that marennine has an
264 ordering effect on *V. splendidus* membrane lipid chains at a concentration of 2 $\mu\text{g}/\text{mL}$, as shown
265 by a 35% increase



267 **Figure 1:** Representative ^2H SS-NMR MAS spectra of *V. splendidus* exposed to marennine
268 during the exponential (a-c) and stationary (d-f) stages. Spectra (a) and (d) are control
269 experiments of *V. splendidus* in ASW; (b) and (e) correspond to bacteria exposed to low
270 marennine (2 $\mu\text{g}/\text{mL}$) concentration; (c) and (f) to marennine at MIC (200 $\mu\text{g}/\text{mL}$). All spectra

271 were recorded at 25°C and normalized with respect to the first spinning sideband to better
 272 highlight the sideband intensity distribution.

273

274 in M_2 value (Table 1). This effect is greater for bacteria sampled in the stationary phase, where M_2
 275 is actually doubled. Figure 1 (b,e) indeed shows that spinning side bands (SSBs) span a larger
 276 frequency range and have increased intensities. The stiffening effect of marennine on the lipid
 277 chains is further observed at the MIC (Table 1). M_2 values increase by 60% compared to the
 278 control in the presence of marennine in the exponential phase and are doubled in the stationary
 279 phase.

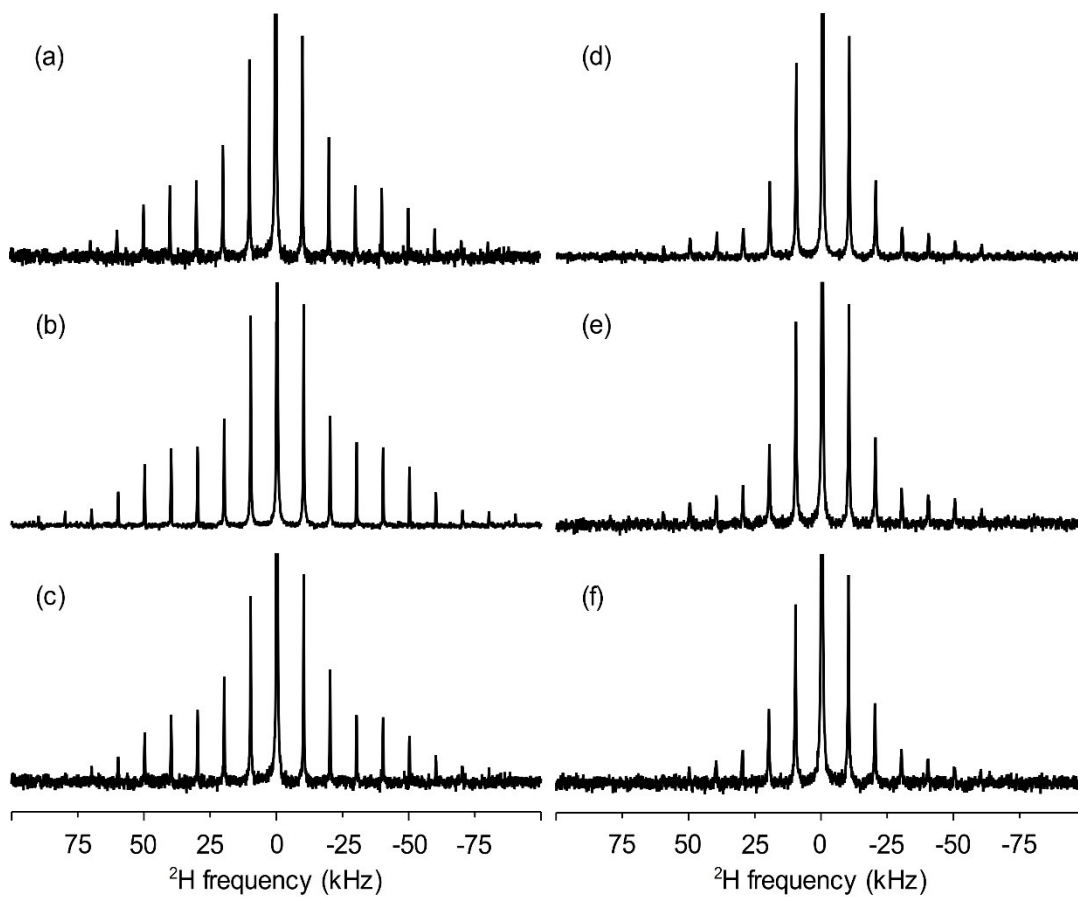
280 **Table 1:** Average second spectral moment, M_2 (10^9 s^{-2}) with standard deviation for *V. splendidus*
 281 exposed to marennine and polymyxin B at different concentrations. MIC for marennine and PxB
 282 are 200 $\mu\text{g/mL}$ and 8 $\mu\text{g/mL}$, respectively. Control for marennine is done in artificial seawater.
 283 All spectra were recorded at 25°C. Standard deviations obtained on three replicates are indicated
 284 between brackets.

	Marennine			Polymyxin B		
	Control	2 $\mu\text{g/mL}$	MIC	Control	1 $\mu\text{g/mL}$	MIC
Exponential phase	25 (5)	34 (7)	39 (4)	20 (2)	23 (3)	18 (3)
Stationary phase	10 (1)	21 (3)	20 (1)	10 (1)	12 (1)	7 (2)

285

286 To explore the marine pigment marennine as a potential antimicrobial agent for aquaculture, its
 287 effect was compared to PxB since polymyxins have been widely used for this purpose. Figure 2
 288 shows the effect of PxB on *V. splendidus* at low concentration (1 $\mu\text{g/mL}$) and at the MIC (8
 289 $\mu\text{g/mL}$). Corresponding M_2 values are presented in Table 1. At low PxB concentration (Figures
 290 2b,e), an small increase in SSB intensities and spectral width can be seen, indicating an increased
 291 lipid chain ordering. Table 1 shows that this moderate increase in lipid ordering at low
 292 concentration of PxB occurs in both the exponential and stationary phase, as revealed by a 15 to
 293 20% increase in M_2 . At the MIC (Figures 2c,f), however, the SSBs intensity is reduced, as well as
 294 the spectral width, with a concomitant decrease in M_2 , revealing a disordering effect of PxB on *V.*
 295 *splendidus* inner membrane lipid chains at both growth phases.

296 With ^2H NMR and M_2 determination, we were also able to provide evidence of the effect of
297 marennine and PxB on *V. splendidus* at different growth times. Control samples were compared
298 to bacteria exposed to each antibacterial agent after a growth period of 15h (mid-log), 22h (early
299 stationary) and 35h (late stationary). Figure 3 shows that M_2 values of *V. splendidus* membranes
300 decrease as a function of the growth stage, in agreement with the increase in membrane fluidity
301 reported in our previous work [22]. The addition of marennine results in an increase in the lipid
302 acyl chain ordering at both concentrations, with a more important effect for bacteria sampled at
303 mid-log phase, compared to the stationary phase (35h of growth). Interestingly, low PxB
304 concentrations increased the membrane rigidity at all growth stages, while high concentration

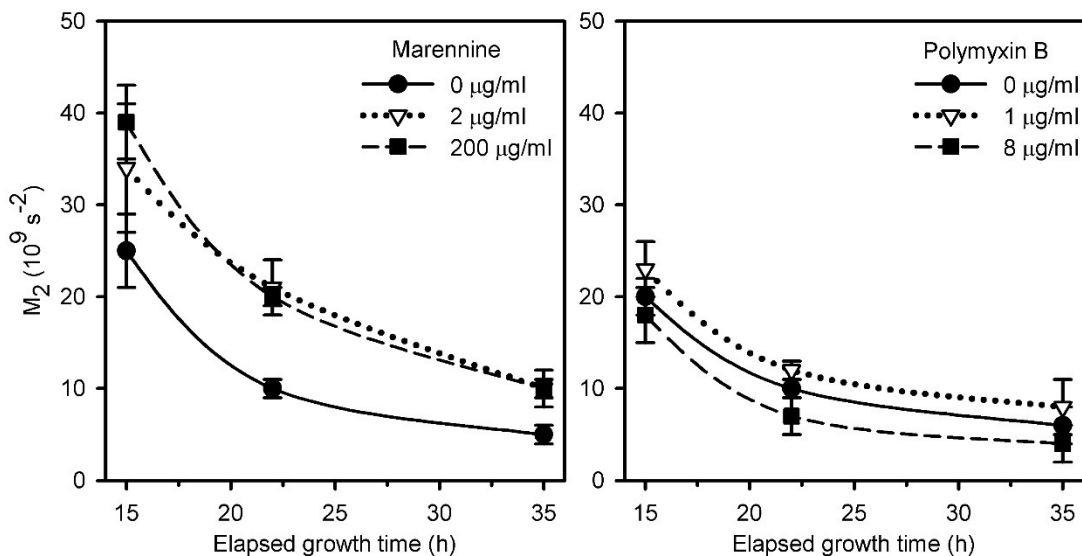


306 **Figure 2:** Representative ^2H SS-NMR MAS spectra of *V. splendidus* exposed to polymyxin B
307 during exponential (a-c) and stationary (d-f) stages. Spectra (a) and (d) are control experiments,
308 spectra (b) and (e) correspond to bacteria exposed to low PxB (1 $\mu\text{g}/\text{mL}$) concentration; (c) and

309 (f) to PxB at MIC (8 $\mu\text{g/mL}$). All spectra were recorded at 25°C and normalized with respect to
310 the first spinning sideband to better highlight the sideband intensity distribution.

311

312 (MIC) showed the opposite pattern. These results are in agreement with an *in vivo* ^2H SS-NMR
313 study of the effect of PxB on the Gram(-) bacterium *E. coli* [19]. They are also compatible with
314 previous work suggesting a two-stage interaction mechanism for this antibiotic with respect to
315 increased concentrations or exposure time [25]. Briefly, PxB first disturbs the bacteria outer
316 membrane by electrostatically binding with the anionic phosphate groups of the
317 lipopolysaccharides (LPS) via its positively charged residues, thus competing with divalent
318 cations such as magnesium and calcium, which play a role in bridging adjacent LPS chains. Then
319 the PxB



321 **Figure 3:** Effect of marennine and PxB on the second spectral moment M_2 of *V. splendidus* after
322 exposure to marennine (left), and PxB (right) at 25°C. Control cells (solid lines) are compared to
323 bacteria exposed to 2 $\mu\text{g/mL}$ of marennine or 1 $\mu\text{g/mL}$ of PxB (dotted lines), and at the respective
324 MICs (dashed lines). Values correspond to average means of three replicates with 3-22% error
325 for marennine samples and 8-40% error for PxB samples.

326 lipid tail can insert itself in the inner membrane, thus disrupting the bilayer, and eventually
327 leading to the loss of membrane integrity and cell leakage [25,26,35]. The importance of LPS is
328 highlighted by the fact that PxB does not significantly affect model membranes made without
329 LPS [36,37].

330 Altogether, these observations suggest that the action mechanism of marennine is similar to
331 that of PxB at low concentration, but different at high concentration. As opposed to PxB,
332 marennine, even at lethal concentrations, would not disrupt the inner bilayer and interact mostly
333 with the outer layer of *V. splendidus* membrane. Nevertheless, while marennine probably does
334 not disrupt the inner membrane, it can still affect it depending on how much it penetrates the
335 outer membrane. To test this hypothesis, we have decided to study the interaction of marennine
336 with *model* inner bacterial membranes.

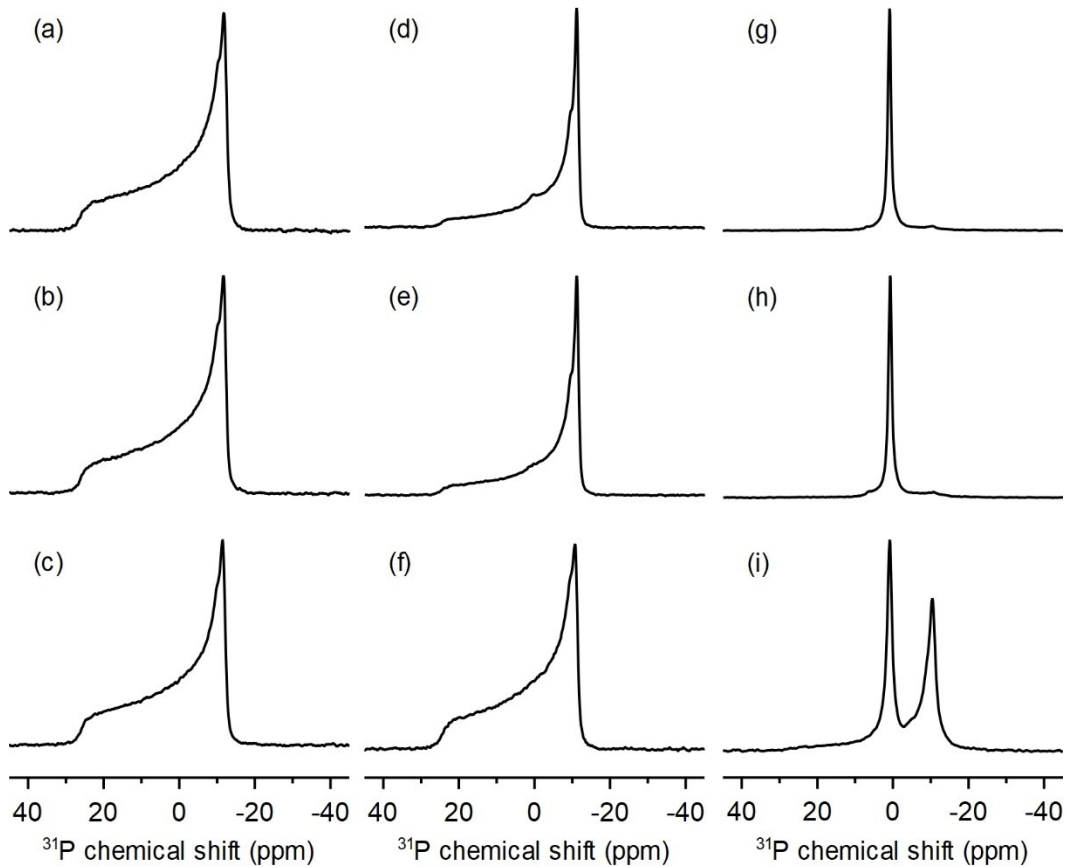
337

338 ***Effect of marennine on model membranes***

339 The ²H SS-NMR results obtained *in vivo* suggest a different action of marennine on *V.*
340 *splendidus*, as compared to PxB, where this natural pigment is shown to reduce the membrane
341 lipid chain dynamics at low concentration and at the MIC, and at both growth stages. Moreover,
342 the action of marennine was observed following a longer incubation time as compared to PxB. To
343 better understand the action mechanism of marennine, we have thus investigated its effect on the
344 lipids using model *V. splendidus* inner membranes, *i.e.*, without LPS. To do so, the phospholipid
345 composition of the bacterium was first determined by ³¹P solution NMR using lipid extracts (a
346 characteristic spectrum is shown in figure S3). Integration of the resonances allowed the
347 quantification of three major phospholipids corresponding to 85% phosphatidylethanolamine
348 (PE), 10% phosphatidylglycerol (PG) and 5% cardiolipin (CL) (in mole %) (phospholipid
349 structures are shown in Figure S3 and the presence of two phosphate headgroups in CL was taken
350 into account in the quantification). These proportions did not change whether samples were
351 harvested at exponential or stationary growth stages. Model membranes (MLVs) of *V. splendidus*
352 were thus prepared using POPE, POPG, and CL, respecting the same proportions as in natural
353 membranes.

354

355 ³¹P SS-NMR is a useful tool to probe changes in phospholipid headgroup dynamics,
356 orientation and lipid phases [38]. The effect of marennine on the model membranes is presented
357 in Figure 4 at low (2 μg/ml) concentration and at the MIC. Spectra were recorded between 25
358 and 75°C to better evidence any possible changes in membrane morphology and phases. First, the
359 model membranes at 25°C and 50°C are typical of bilayers in liquid-crystalline phase, with a
360 chemical shift anisotropy (CSA, powder spectrum width) of approximately 37.5 and 33 ppm,
361 respectively. The higher intensity of the right edge of the powder spectrum at 50°C can be
362 explained by a change in liposomes from a spherical to an ellipsoidal shape, as confirmed by
363 spectral simulation (Figure S4). Indeed, the ratio ρ between the long and short axis of the
364 liposomes changes from that of a sphere (ρ=1) to an ellipsoid (ρ=1.5) from 25 to 50°C. This is
365 explainable by the collective orientation of the phospholipids in a fluid membrane in the
366 magnetic field, due to their negative magnetic susceptibility anisotropy [39,40]. At 75°C, the
367 spectrum shows a narrow and symmetric high intensity line and a residual powder pattern.
368 Importantly, when the temperature was reduced, the spectra were identical to those before heating
369 and therefore the isotropic peak does not result from lipid degradation. Bilayers are thus mostly
370 transformed into smaller fast tumbling structures (67%



372 **Figure 4:** ^{31}P -SS NMR spectra of model *V. splendidus* membranes as a function of temperature:
 373 (a-c) $T=25^\circ\text{C}$, (d-f) $T=50^\circ\text{C}$ and (g-i) $T=75^\circ\text{C}$. Top three spectra (a,d and g) are controls without
 374 marennine, middle spectra (b,e and h) are at a marennine concentration of $2\ \mu\text{g/mL}$, and bottom
 375 spectra (c,f and i) are at the MIC ($200\ \mu\text{g/mL}$). Note the lineshape difference between spectra d
 376 and e which could be fitted with a ratio of long to short ellipsoid axis of $\rho=1.5$ compared to the
 377 more spherical cases (a-c, f) with $\rho=1$ as calculated by spectral simulations.

378

379 of the spectrum area, Table 2). It should be noted that the isotropic signal may also result from
 380 lipid lateral diffusion in a highly curved bilayer and non-bilayer lipid structures [41]. **DOPE, the**
 381 **most abundant lipid (85%) in our model membranes, is known to adopt a hexagonal phase at high**
 382 **temperatures. However, such phase could not be observed on the spectra at all temperatures most**
 383 **likely due to the presence of PG and CL. Indeed, Warschawski *et al.* [42] reported that only 20%**
 384 **of PG in a PG/PE mixture can govern the phase behaviour of the membranes at 75°C . Under our**

385 **Table 2:** Estimated phase contributions expressed in % from area integration of *V. splendidus*
 386 model membranes at 75°C, in the absence and presence of marennine at two concentrations.
 387 Standard deviations **obtained on three replicates** are indicated between brackets.

	Marennine		
	Control	2 µg/mL	MIC
Isotropic phase	87% (8)	79% (6)	33% (8)
Lamellar phase	13% (8)	21% (6)	67% (8)

388
 389 **conditions, with only 10% PG in the mixture, CL seems to contribute to maintaining a lamellar**
 390 **phase, as it is known to exert a major stabilizing effect on zwitterionic lipids [42,43].**

391 The effect of marennine on the phospholipid headgroups of *V. splendidus* model membranes
 392 seems to depend on the concentration and temperature. At 25°C, Figure 4 shows no effect at both
 393 pigment concentrations. However, at 50°C, high concentrations of marennine re-establish the
 394 initial spherical shape of the MLVs, with going from 1.5 to 1 in the presence of the pigment.
 395 **These observations suggest that marennine increases the rigidity of the membrane and lipid**
 396 **liposomes therefore become harder to deform. This result is consistent with the increase in ²H M2**
 397 **observed on the bacteria.** Previous studies have reported that compounds such as antimicrobial
 398 peptides [44-46] or phenolic molecules [47] can have a similar action, *i.e.*, altering the
 399 membranes without necessarily changing the CSA value. The interaction of marennine would
 400 thus impede the temperature-induced fast lateral diffusion and motion of the lipid polar
 401 headgroups, as was, for example, reported for proteins interacting with DMPC (1,2-
 402 dipalmitoylphosphatidylcholine) membranes [48]. **An alternative explanation could be that**
 403 **marennine, with an anisotropy of diamagnetic susceptibility of opposing sign to the one of the**
 404 **lipids, would counter the field-induced deformation of the membrane. However, since the exact**
 405 **structure of marennine is unknown, this is for the moment a simple hypothesis.** At 75°C and in
 406 the presence of 200 µg/mL, lipids are mostly found in a lamellar phase (67%) as shown in Table
 407 2, as compared to about 10% in the control sample. Altogether, our results suggest that
 408 marennine protects the lamellar phase.

409 The weak effects of marennine on the model bacterial membranes are comparable to those of
 410 negatively charged molecules observed on membrane systems [45,49]. Reported effects of

411 anionic molecules on zwitterionic membranes include alterations of lipid packing and gelation
412 [50], vesicle shrinkage [50], or aggregation, as a result of hydration or condensation of the acyl
413 chains [51]. The model *V. splendidus* membranes used in our work are composed of zwitterionic
414 PE and anionic PG and CL (Figure S3). It is possible that the negative charges of marennine
415 interact with PE's positive amine group, while the hydroxyl groups of the pigment form H-bonds
416 with PG and CL, similarly to polyhydroxylated fullerene (fullerenol) nanoparticles which were
417 shown to selectively interact with PG in model membranes, and remain at the lipid/water
418 interface [52].

419

420 ***Interaction mechanism of marennine with V. splendidus***

421 The outer membrane of *Vibrio* species is extremely selective, blocking the permeation of
422 molecules greater than 600-700 Da [53]. A 10-kDa molecule such as marennine is therefore
423 unlikely to traverse the outer membrane. The great diversity in responses to marennine exposure
424 observed with different species and strains of *Vibrio*, ranging from growth stimulation to
425 complete inhibition, could thus originate from molecule specificity and diversity at the bacterial
426 membrane level [17]. Our model membrane study reveals that, if marennine penetrated the outer
427 membrane and reached the inner membrane, it would only weakly perturb the ³¹P atom vicinity,
428 consistent with the absence of change in CSA. It would also slightly affect the membrane elastic
429 properties, consistent with the stiffening effect observed by ²H SS-NMR. The results obtained by
430 ³¹P SS-NMR using MLVs highlight the importance of marennine's charged and hydroxylated
431 groups upon molecular interactions, and help understanding the stiffening effect of marennine
432 observed by ²H SS-NMR *in vivo* with *V. splendidus*.

433 Altogether, our results confirm our initial hypothesis that, as opposed to PxB, and even at
434 concentrations at which marennine inhibits bacterial growth, marennine does not disrupt bacterial
435 membranes. Marennine most likely interacts with the LPS on the bacterium outer membrane, as
436 was suspected with *E. coli* [19]. Similarly, Tardy-Laporte *et al.* studied the effect of fullerenol
437 nanoparticles on *E. coli*, and hypothesized that the membrane stiffening effect of this
438 polyhydroxylated molecule was due to an interaction with the polysaccharide core of the LPS,
439 thus inducing a tighter packing of the phospholipids in the outer leaflet of the outer membrane
440 [19]. A similar effect to fullerenol is thus suspected for marennine towards *V. splendidus*.

441 While a direct interaction of marennine can explain this membrane stiffening, the implication
442 of other biochemical mechanisms cannot be ruled out. Under stress situations such as the
443 presence of toxic organic compounds or nutrient deprivation, *Vibrio* species can react by
444 rigidifying their outer membrane, for example via a *cis-trans* conversion process within the lipid
445 unsaturated fatty acids [54,55]. These isomerizations have been reported to increase with
446 increasing phenol concentrations [56], aligning with the increased effect of marennine at the
447 MIC, which may suggest increased phospholipid recruitment for isomerization. If marennine can
448 hardly traverse *V. splendidus* outer membrane, it could still interfere with bacterial outer
449 membrane proteins and induce such rearrangement at the membrane level. Indeed, it has been
450 observed *in vitro* that marennine can interact with and precipitate proteins, a similar effect to that
451 of polyphenols (Mouget, unpublished results). Stiffening could also be induced by cell shrinking
452 due to lower water permeability under stress conditions [57].

453 Functional consequences of membrane fluidity alteration by marennine are enough to affect
454 bacterial viability, as it may involve the perturbation of lipid-protein domains, and affect
455 processes such as biofilm formation, cytokinesis or enzymatic pathways [58,59]. More
456 specifically, for virulent bacteria under stress, the release of chemical molecules during quorum
457 sensing process could be directly affected by the alteration of membrane fluidity [60].

458

459 CONCLUSION

460 In this work, the action of marennine towards the marine bacterium *V. splendidus* was studied
461 for the first time, at the molecular level, by *in vivo* ^2H SS-NMR, at different growth phases. The
462 antibiotic PxB was used as a reference antibiotic acting against Gram(-) bacteria. While PxB was
463 proved efficient against infection threats in aquaculture, nowadays' regulations as well as
464 increased bacteria resistance prompt more natural alternatives. Our study demonstrates that
465 marennine affects *V. splendidus* membranes at low concentrations, below the MIC. This
466 microalgal pigment, which is not harmful for humans, could thus constitute a potential treatment
467 against vibriosis. Our results also showed that marennine and PxB act against this bacterium via
468 different mechanisms. As proposed in other studies [25,26,35], PxB would disturb the bacteria
469 outer membrane before accessing and disrupting the inner membrane. However, marennine
470 would act in the vicinity of *V. splendidus* outer membrane through a stiffening mechanism.
471 Marennine could interact with the LPS in the outer membrane, and/or trigger the isomerization of

472 unsaturated fatty acids, as a stress-resistance reaction. More investigations would be required to
473 test these hypotheses.

474 Finally, our results indicate that both marennine and PxB had a stronger effect in the stationary
475 phase than in the exponential phase. Beney and Gervais [61] have reported that the membrane
476 capacity to resist a source of stress by increasing the lipid ordering is highly related to the initial
477 membrane fluidity state during cell growth. As shown in our previous study [22], cell membranes
478 are more fluid in the stationary phase as compared to the mid-log phase, which would explain the
479 more dramatic stiffening effect of the antimicrobial agents observed in the stationary phase. In all
480 cases, results showed herein indicate that the membrane stiffening induced by marennine occurs
481 even in balanced healthy stage cultures of *V. splendidus* (exponential phase), suggesting that this
482 natural pigment is a potential candidate for antibacterial treatment in aquaculture.

483

484 **ACKNOWLEDGMENTS**

485 We would like to thank Pierre Audet for sharing the MestRenova macro, François Turcotte for
486 marennine production and purification, and Karine Lemarchand (ISMER) for providing the initial
487 *Vibrio* strain. This work was supported by the Natural Sciences and Engineering Research
488 Council (NSERC) of Canada (grant 326750-2013 to I.M. and grant 299100 to R.T.) and the
489 Centre National de la Recherche Scientifique (UMR 7203 to D.E.W.). This publication also
490 benefited from the Horizon 2020 Research and Innovation Programme GHaNA (The Genus
491 *Haslea*, New marine resources for blue biotechnology and Aquaculture) under Grant Agreement
492 No. 734708/GHANA/H2020-MSCA-RISE-2016 (J.-L.M). Z.B. would like to acknowledge the
493 Government of Tunisia and Ressources Aquatiques Québec (RAQ) research network from the
494 Fonds de recherche Nature et technologie FRQNT (RS-171172) for the award of scholarships.
495 I.M., J.-L.M., J-S.D. and R.T. are members of RAQ.

496 **COMPETING INTERESTS**

497 No competing interests declared.

498 **AUTHOR CONTRIBUTIONS**

499 Z.B. designed and conducted all sampling, data collection and analysis, and wrote the first draft
500 of the manuscript. J-S.D. monitored microalgal culture, performed marennine production and
501 purification, and participated in the revision of the manuscript. J-L.M. provided the initial *Haslea*

502 strain culture and participated in the revision of the manuscript. A.A.A. and D.E.W assisted with
503 NMR operation and analysis, and participated in the revision of the manuscript. R.T. and I.M.
504 designed and supervised the research, contributed to the data analysis and writing of the
505 manuscript.

506 REFERENCES

507

508 [1] A.G.J. Tacon, Global trends in aquaculture and compound aquafeed production, in: World
509 Aquaculture Magazine, vol. 49, World Aquaculture Society, Los Angeles, 2018, pp. 33-46.

510 [2] C. Paillard, F. Le Roux, J.J. Borrego, Bacterial disease in marine bivalves, a review of recent
511 studies: trends and evolution, *Aquat. Living Resour.*, 17 (2004) 477-498.

512 [3] R.A. Raja, K. Jithendran, Aquaculture disease diagnosis and health management, in: S.
513 Perumal, A.R. Thirunavukkarasu, P. Perumal (Eds.) *Advances in Marine and Brackishwater*
514 *Aquaculture*, Springer, 2015, pp. 247-255.

515 [4] F.L. Thompson, T. Iida, J. Swings, Biodiversity of Vibrios, *Microbiol. Mol. Biol. Rev.*, 68
516 (2004) 403-431.

517 [5] L. DiSalvo, J. Blecka, R. Zebal, *Vibrio anguillarum* and larval mortality in a California
518 coastal shellfish hatchery, *Appl. Environ. Microbiol.*, 35 (1978) 219-221.

519 [6] M.-A. Travers, K.B. Miller, A. Roque, C.S. Friedman, Bacterial diseases in marine bivalves,
520 *J. Invertebr. Pathol.*, 131 (2015) 11-31.

521 [7] M. Holbach, R. Robert, P. Boudry, B. Petton, P. Archambault, R. Tremblay, Scallop larval
522 survival from erythromycin treated broodstock after conditioning without sediment, *Aquaculture*,
523 437 (2015) 312-317.

524 [8] J.E. Watts, H.J. Schreier, L. Lanska, M.S. Hale, The rising tide of antimicrobial resistance in
525 aquaculture: sources, sinks and solutions, *Mar. drugs*, 15 (2017) 158.

526 [9] M. Weir, A. Rajić, L. Dutil, C. Uhland, N. Bruneau, Zoonotic bacteria and antimicrobial
527 resistance in aquaculture: opportunities for surveillance in Canada, *Can. Vet. J.*, 53 (2012) 619.

528 [10] F.C. Cabello, Heavy use of prophylactic antibiotics in aquaculture: a growing problem for
529 human and animal health and for the environment, *Environmental microbiology*, 8 (2006) 1137-
530 1144.

531 [11] T. Defoirdt, P. Sorgeloos, P. Bossier, Alternatives to antibiotics for the control of bacterial
532 disease in aquaculture, *Curr. Opin. Microbiol.*, 14 (2011) 251-258.

533 [12] A. Ravi, K. Musthafa, G. Jegathammbal, K. Kathiresan, S. Pandian, Screening and
534 evaluation of probiotics as a biocontrol agent against pathogenic Vibrios in marine aquaculture,
535 *Lett. Appl. Microbiol.*, 45 (2007) 219-223.

536 [13] R. Gastineau, F. Turcotte, J.-B. Pouvreau, M. Morançais, J. Fleurence, E. Windarto, F.
537 Prasetya, S. Arsad, P. Jaouen, M. Babin, L. Coiffard, C. Couteau, J.-F. Bardeau, B. Jacqueline, V.
538 Leignel, Y. Hardivillier, I. Marcotte, N. Bourgougnon, R. Tremblay, J.-S. Deschênes, H.
539 Badawy, P. Pasetto, N. Davidovich, G. Hansen, J. Dittmer, J.-L. Mouget, Marennine, promising
540 blue pigments from a widespread *Haslea* diatom species complex, *Mar. drugs*, 12 (2014) 3161-
541 3189.

542 [14] F. Turcotte, J.-L. Mouget, B. Genard, K. Lemarchand, J.-S. Deschênes, R. Tremblay,
543 Prophylactic effect of *Haslea ostrearia* culture supernatant containing the pigment marennine to
544 stabilize bivalve hatchery production, *Aquat. Living Resour.*, 29 (2016) 401.

545 [15] J.-B. Pouvreau, M. Morançais, F. Fleury, P. Rosa, L. Thion, B. Cahingt, F. Zal, J. Fleurence,
546 P. Pondaven, Preliminary characterisation of the blue-green pigment “marennine” from the
547 marine tychopelagic diatom *Haslea ostrearia* (Gaillon/Bory) Simonsen, *J. Appl. Phycol.*, 18
548 (2006) 757-767.

549 [16] C. Falaise, P. Cormier, R. Tremblay, C. Audet, J.-S. Deschênes, F. Turcotte, C. François, A.
550 Seger, G. Hallegraeff, N. Lindquist, D. Sirjacobs, S. Gobert, P. Lejeune, V. Demoulin, J.-L.
551 Mouget, Harmful or harmless: Biological effects of marennine on marine organisms, *Aquat.*
552 *Toxicol.*, 209 (2019) 13-25.

553 [17] C. Falaise, A. James, M.-A. Travers, M. Zanella, M. Badawi, J.-L. Mouget, Complex
554 Relationships between the Blue Pigment Marennine and Marine Bacteria of the Genus *Vibrio*,
555 *Mar. Drugs*, 17 (2019) 160.

556 [18] R. Gastineau, J.-B. Pouvreau, C. Hellio, M. Morançais, J.I. Fleurence, P. Gaudin, N.
557 Bourgougnon, J.-L. Mouget, Biological activities of purified marennine, the blue pigment
558 responsible for the greening of oysters, *J. Agric. Food Chem.*, 60 (2012) 3599-3605.

559 [19] C. Tardy-Laporte, A.A. Arnold, B. Genard, R. Gastineau, M. Morançais, J.-L. Mouget, R.
560 Tremblay, I. Marcotte, A ²H solid-state NMR study of the effect of antimicrobial agents on intact
561 *Escherichia coli* without mutating, *Biochim. Biophys. Acta, Biomembr.*, 1828 (2013) 614-622.

562 [20] M. Laadhari, A.A. Arnold, A.E. Gravel, F. Separovic, I. Marcotte, Interaction of the
563 antimicrobial peptides caerin 1.1 and aurein 1.2 with intact bacteria by ²H solid-state NMR,
564 *Biochim. Biophys. Acta, Biomembr.*, 1858 (2016) 2959-2964.

565 [21] X.L. Warnet, M. Laadhari, A.A. Arnold, I. Marcotte, D.E. Warschawski, A ²H magic-angle
566 spinning solid-state NMR characterisation of lipid membranes in intact bacteria, *Biochim.*
567 *Biophys. Acta, Biomembr.*, 1858 (2016) 146-152.

568 [22] Z. Bouhrel, A.A. Arnold, D.E. Warschawski, K. Lemarchand, R. Tremblay, I. Marcotte,
569 Labelling strategy and membrane characterization of marine bacteria *Vibrio splendidus* by *in vivo*
570 ²H NMR, *Biochim. Biophys. Acta, Biomembr.*, 1861 (2019) 871-878.

571 [23] V. Booth, D.E. Warschawski, N.P. Santisteban, M. Laadhari, I. Marcotte, Recent progress
572 on the application of ²H solid-state NMR to probe the interaction of antimicrobial peptides with
573 intact bacteria, *Biochim. Biophys. Acta, Proteins Proteomics*, 1865 (2017) 1500-1511.

574 [24] P.H. Serrano, Responsible use of antibiotics in aquaculture, in, FAO, Rome, 2005, pp. 97.

575 [25] Z.Z. Deris, J.D. Swarbrick, K.D. Roberts, M.A. Azad, J. Akter, A.S. Horne, R.L. Nation,
576 K.L. Rogers, P.E. Thompson, T. Velkov, Probing the penetration of antimicrobial polymyxin
577 lipopeptides into Gram-negative bacteria, *Bioconjugate Chem.*, 25 (2014) 750-760.

578 [26] A. Clausell, M. Pujol, M. Alsina, Y. Cajal, Influence of polymyxins on the structural
579 dynamics of *Escherichia coli* lipid membranes, *Talanta*, 60 (2003) 225-234.

580 [27] D.R. Mateo, A. Siah, M.T. Araya, F.C. Berthe, G.R. Johnson, S.J. Greenwood, Differential
581 *in vivo* response of soft-shell clam hemocytes against two strains of *Vibrio splendidus*: changes in
582 cell structure, numbers and adherence, *J. Invertebr. Pathol.*, 102 (2009) 50-56.

583 [28] K. Yoshida, Y. Mukai, T. Niidome, C. Takashi, Y. Tokunaga, T. Hatakeyama, H. Aoyagi,
584 Interaction of pleurocidin and its analogs with phospholipid membrane and their antibacterial
585 activity, *J. Pept. Res.*, 57 (2001) 119-126.

586 [29] J. Folch, M. Lees, G.H. Sloane Stanley, A simple method for the isolation and purification
587 of total lipides from animal tissues, *J. Biol. Chem.*, 226 (1957) 497-509.

588 [30] Y. Marty, F. Delaunay, J. Moal, J.F. Samain, Changes in the fatty acid composition of
589 *Pecten maximus* (L.) during larval development, *J. Exp. Mar. Biol. Ecol.*, 163 (1992) 221-234.

590 [31] M.A. Dubinnyi, D.M. Lesovoy, P.V. Dubovskii, V.V. Chupin, A.S. Arseniev, Modeling of
591 ³¹P-NMR spectra of magnetically oriented phospholipid liposomes: A new analytical solution,
592 Solid State Nucl. Magn. Reson., 29 (2006) 305-311.

593 [32] T. Taguri, T. Tanaka, I. Kouno, Antimicrobial activity of 10 different plant polyphenols
594 against bacteria causing food-borne disease, Biol. Pharm. Bull., 27 (2004) 1965-1969.

595 [33] V. Razafintsalama, S. Sarter, L. Mambu, R. Randrianarivo, T. Petit, J.F. Rajaonarison, C.
596 Mertz, D. Rakoto, V. Jeannoda, Antimicrobial activities of *Dilobeia thouarsii* Roemer and
597 Schulte, a traditional medicinal plant from Madagascar, S. Afr. J. Bot., 87 (2013) 1-3.

598 [34] M. Vaara, Polymyxins and their novel derivatives, Curr. Opin. Microbiol., 13 (2010) 574-
599 581.

600 [35] A.H. Delcour, Outer membrane permeability and antibiotic resistance, Biochim. Biophys.
601 Acta, Proteins Proteomics, 1794 (2009) 808-816.

602 [36] F. Sixl, A. Watts, Deuterium and phosphorus nuclear magnetic resonance studies on the
603 binding of polymyxin B to lipid bilayer-water interfaces, Biochemistry, 24 (1985) 7906-7910.

604 [37] R. Zidovetzki, U. Banerjee, D.W. Harrington, S.I. Chan, NMR study of the interactions of
605 polymyxin B, gramicidin S, and valinomycin with dimyristoyllecithin bilayers, Biochemistry, 27
606 (1988) 5686-5692.

607 [38] J. Seelig, ³¹P nuclear magnetic resonance and the head group structure of phospholipids in
608 membranes, Biochim. Biophys. Acta, Rev. Biomembr., 515 (1978) 105-140.

609 [39] I. Marcotte, A. Bélanger, M. Auger, The Orientation Effect of Gramicidin A on Bicelles and
610 Eu³⁺-Doped Bicelles as Studied by Solid-State NMR and FTIR Spectroscopy, Chem. Phys.
611 Lipids, 139 (2006) 137-149.

612 [40] F. Picard, M.-J. Paquet, J. Levesque, A. Bélanger, M. Auger, ³¹P NMR first spectral moment
613 study of the partial magnetic orientation of phospholipid membranes, Biophys. J., 77 (1999) 888-
614 902.

615 [41] P.t. Cullis, B.d. Kruijff, Lipid polymorphism and the functional roles of lipids in biological
616 membranes, Biochim. Biophys. Acta, Rev. Biomembr., 559 (1979) 399-420.

617 [42] B. De Kruijff, P. Cullis, Cytochrome c specifically induces non-bilayer structures in
618 cardiolipin-containing model membranes, Biochim. Biophys. Acta, Biomembr., 602 (1980) 477-
619 490.

620 [43] R.N. Lewis, R.N. McElhaney, The physicochemical properties of cardiolipin bilayers and
621 cardiolipin-containing lipid membranes, Biochim. Biophys. Acta, Biomembr., 1788 (2009) 2069-
622 2079.

623 [44] J.-X. Lu, K. Damodaran, J. Blazyk, G.A.J.B. Lorigan, Solid-state nuclear magnetic
624 resonance relaxation studies of the interaction mechanism of antimicrobial peptides with
625 phospholipid bilayer membranes, Biochemistry, 44 (2005) 10208-10217.

626 [45] S. Thennarasu, D.-K. Lee, A. Poon, K.E. Kawulka, J.C. Vederas, A. Ramamoorthy,
627 Membrane permeabilization, orientation, and antimicrobial mechanism of subtilisin A, Chem.
628 Phys. Lipids, 137 (2005) 38-51.

629 [46] É. Robert, T. Lefèvre, M. Fillion, B. Martial, J. Dionne, M. Auger, Mimicking and
630 understanding the agglutination effect of the antimicrobial peptide thanatin using model
631 phospholipid vesicles, Biochemistry, 54 (2015) 3932-3941.

632 [47] S. Fujisawa, Y. Kadoma, Y. Komoda, ¹H and ¹³C NMR studies of the interaction of eugenol,
633 phenol, and triethyleneglycol dimethacrylate with phospholipid liposomes as a model system for
634 odontoblast membranes, J. Dent. Res., 67 (1988) 1438-1441.

635 [48] S. Rajan, S.-Y. Kang, H.S. Gutowsky, E. Oldfield, Phosphorus nuclear magnetic resonance
636 study of membrane structure. Interactions of lipids with protein, polypeptide, and cholesterol, J.
637 Biol. Chem., 256 (1981) 1160-1166.

638 [49] B. Wang, L. Zhang, S.C. Bae, S. Granick, Nanoparticle-induced surface reconstruction of
639 phospholipid membranes, Proc. Natl. Acad. Sci., 105 (2008) 18171-18175.

640 [50] D. Grillo, M. Olvera de la Cruz, I. Szleifer, Theoretical studies of the phase behavior of
641 DPPC bilayers in the presence of macroions, Soft Matter, 7 (2011) 4672-4679.

642 [51] M.A. Morini, M.B. Sierra, V.I. Pedroni, L.M. Alarcon, G.A. Appignanesi, E.A. Disalvo,
643 Influence of temperature, anions and size distribution on the zeta potential of DMPC, DPPC and
644 DMPE lipid vesicles, Colloids Surf. B 131 (2015) 54-58.

645 [52] P.P. Brisebois, A.A. Arnold, Y.M. Chabre, R. Roy, I. Marcotte, Comparative study of the
646 interaction of fullerene nanoparticles with eukaryotic and bacterial model membranes using
647 solid-state NMR and FTIR spectroscopy, Eur. Biophys. J., 41 (2012) 535-544.

648 [53] F.C. Neidhardt, J.L. Ingraham, M. Schaechter, J.-P. Bohin, Physiologie de la cellule
649 bactérienne: une approche moléculaire, Dunod, 1994.

650 [54] N. Morita, A. Shibahara, K. Yamamoto, K. Shinkai, G. Kajimoto, H. Okuyama, Evidence
651 for cis-trans isomerization of a double bond in the fatty acids of the psychrophilic bacterium
652 *Vibrio sp.* strain ABE-1, J. Bacteriol., 175 (1993) 916-918.

653 [55] H.J. Heipieper, F. Meinhardt, A. Segura, The cis-trans isomerase of unsaturated fatty acids
654 in *Pseudomonas* and *Vibrio*: biochemistry, molecular biology and physiological function of a
655 unique stress adaptive mechanism, FEMS Microbiol. Lett., 229 (2003) 1-7.

656 [56] R. Diefenbach, H.-J. Heipieper, H. Keweloh, The conversion of cis into trans unsaturated
657 fatty acids in *Pseudomonas putida* P8: evidence for a role in the regulation of membrane fluidity,
658 Appl. Microbiol. Biotechnol., 38 (1992) 382-387.

659 [57] E.E. Tymczynszyn, A. Gómez-Zavaglia, E.A. Disalvo, Influence of the growth at high
660 osmolality on the lipid composition, water permeability and osmotic response of *Lactobacillus*
661 *bulgaricus*, Arch. Biochem. Biophys., 443 (2005) 66-73.

662 [58] M. Daglia, Polyphenols as antimicrobial agents, Curr. Opin. Biotechnol., 23 (2012) 174-181.

663 [59] A.-N. Li, S. Li, Y.-J. Zhang, X.-R. Xu, Y.-M. Chen, H.-B. Li, Resources and biological
664 activities of natural polyphenols, Nutrients, 6 (2014) 6020-6047.

665 [60] C. Baysse, M. Cullinane, V. Denervaud, E. Burrowes, J.M. Dow, J.P. Morrissey, L. Tam,
666 J.T. Trevors, F. O'Gara, Modulation of quorum sensing in *Pseudomonas aeruginosa* through
667 alteration of membrane properties, Microbiology, 151 (2005) 2529-2542.

668 [61] L. Beney, P. Gervais, Influence of the fluidity of the membrane on the response of
669 microorganisms to environmental stresses, Appl. Microbiol. Biotechnol., 57 (2001) 34-42.

670

671 Supplementary Materials for

672

673 **Investigating the action of the microalgal pigment marennine on *Vibrio***
674 ***splendidus* by *in vivo* ^2H and ^{31}P solid-state NMR**

675 *Zeineb Bouhlel^{1,2}, Alexandre A. Arnold², Jean-Sébastien Deschênes³ Jean-Luc Mouget⁴, Dror E.*
676 *Warschawski^{2,5}, Réjean Tremblay¹ and Isabelle Marcotte^{2*}*

677

678 ¹ Institut des Sciences de la Mer de Rimouski, Université du Québec à Rimouski, G5L 3A1,
679 Rimouski, Canada

680

681 ² Department of Chemistry, Université du Québec à Montréal, P.O. Box 8888, Downtown
682 Station, H3C 3P8, Montreal, Canada

683

684 ³ Mathematics, computer science and engineering department, Université du Québec à Rimouski,
685 G5L 3A1, Rimouski, Canada.

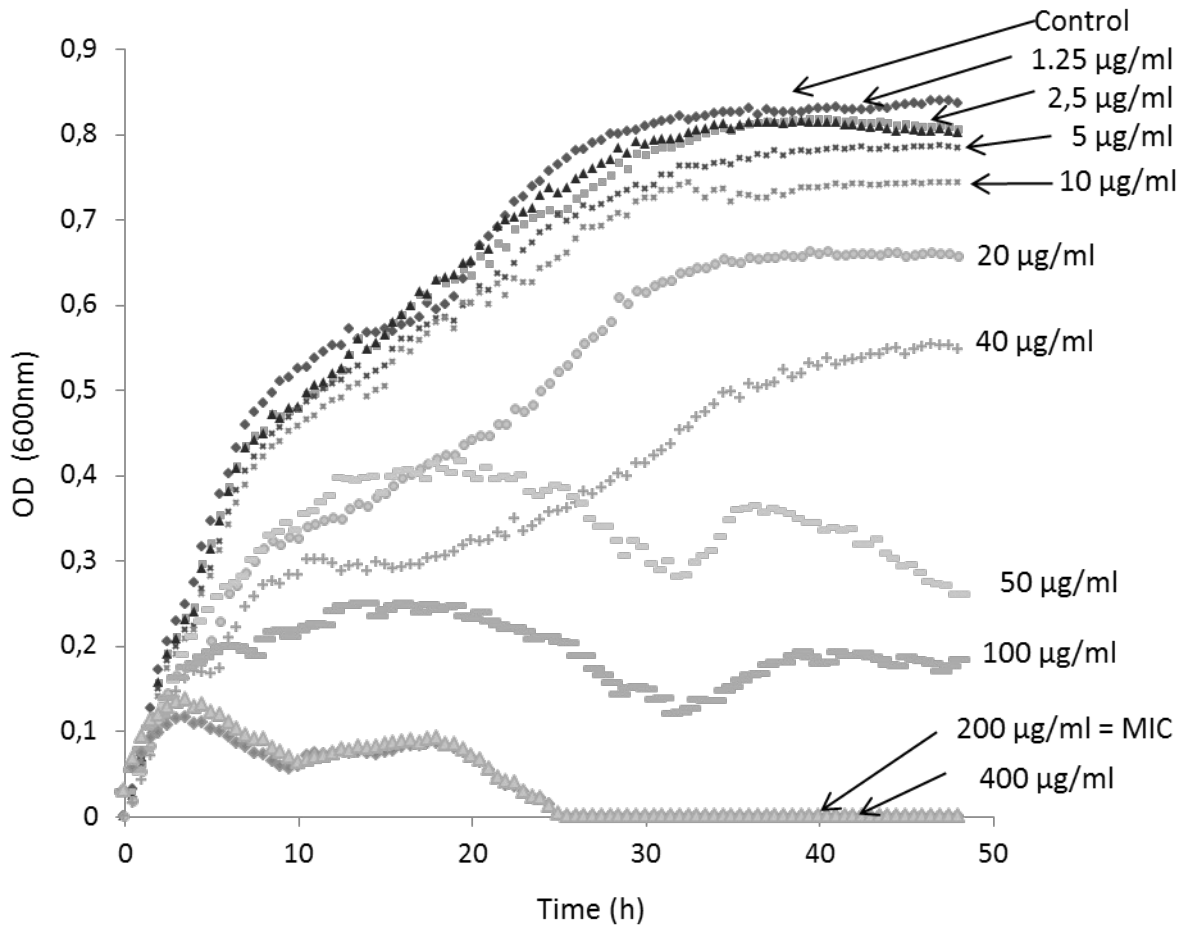
686

687 ⁴ Mer-Molécules-Santé, MMS, FR CNRS 3473, IUML, Le Mans Université, 72000 Le Mans,
688 France

689

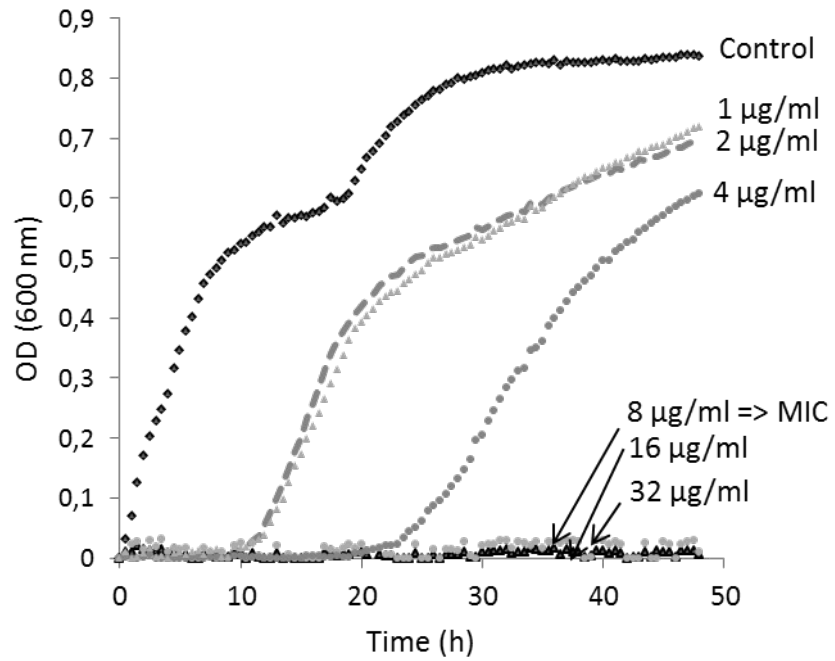
690 ⁵ Laboratoire des Biomolécules, LBM, CNRS UMR 7203, Sorbonne Université, École normale
691 supérieure, PSL University, 75005 Paris, France

692



693

694 **Figure S1:** Determination of minimal inhibitory concentration (MIC) for marennine with
 695 bacterial growth (OD = 600nm) as a function of time (hours). MIC is indicated.

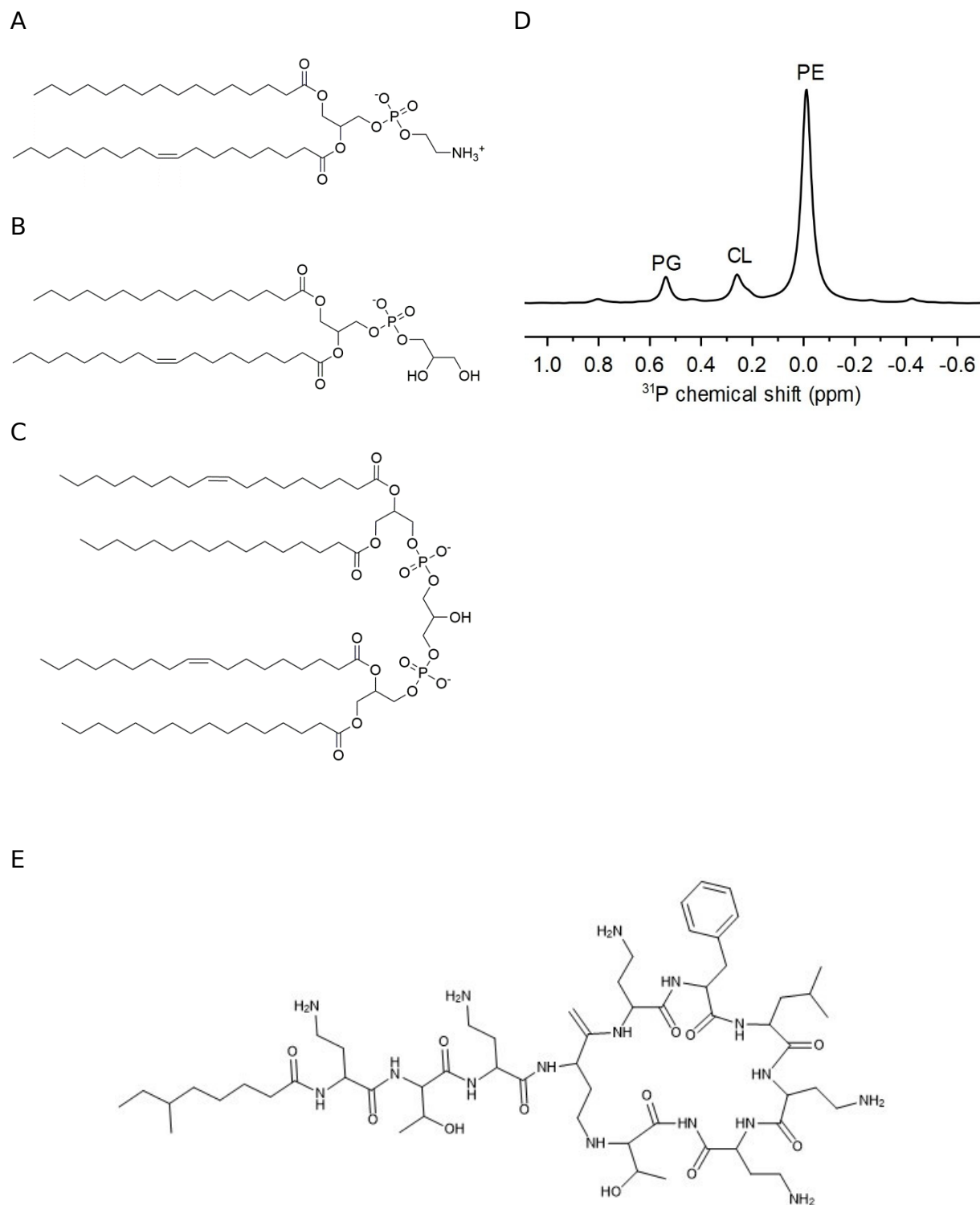


696

697 **Figure S2:** Determination of minimal inhibitory concentration (MIC) for polymyxin B with
 698 bacterial growth (OD = 600nm) as a function of time (hours). MIC is indicated.

699

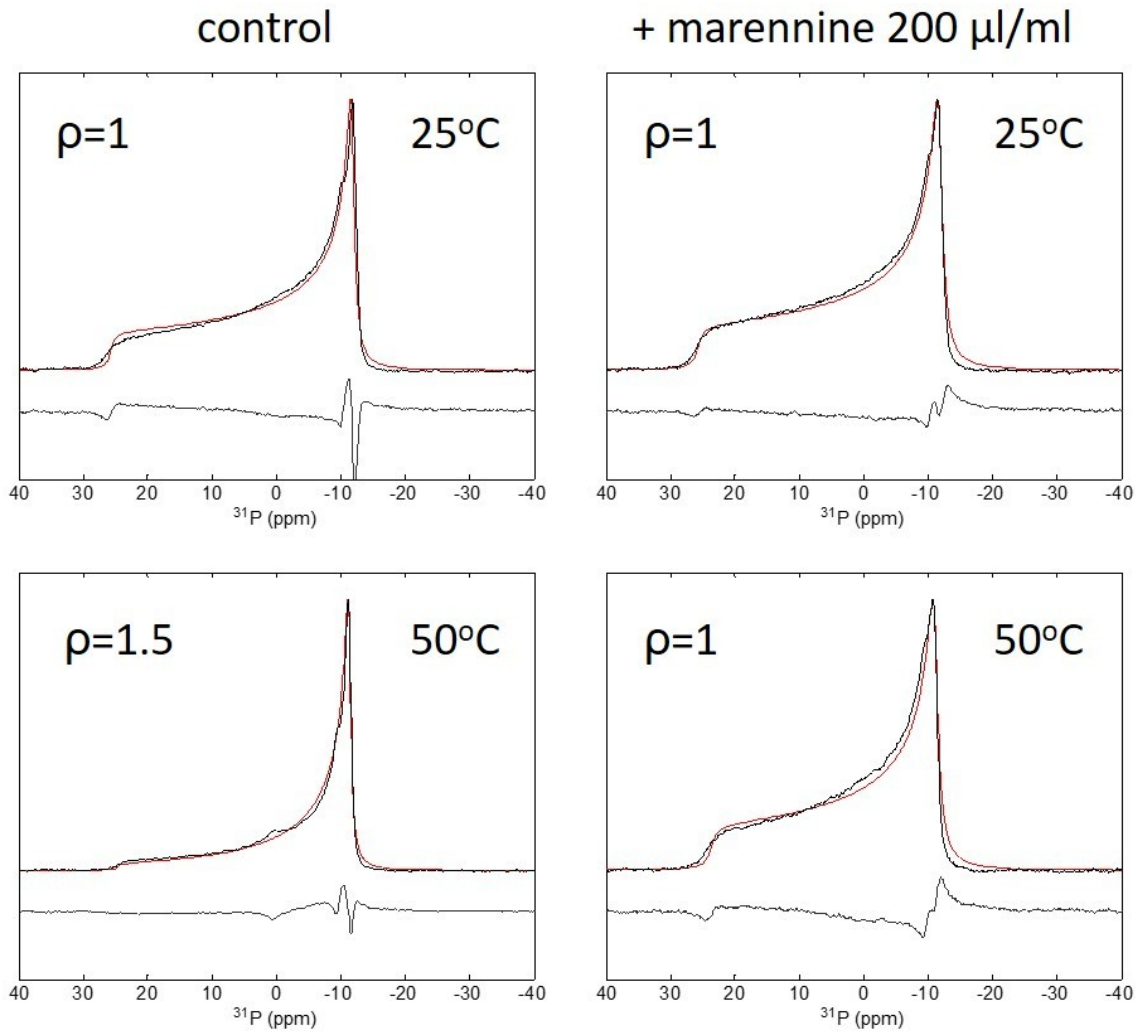
700



701

702 **Figure S3:** Chemical structures of phospholipids used in model membranes of *V. splendidus*. A:
 703 phosphatidylethanolamine (PE), B: phosphatidylglycerol (PG) and C: cardiolipin (CL). D:
 704 Characteristic ^{31}P solution NMR spectrum of lipid extracts of *V. splendidus* (7SHRW) grown in

705 LB medium at 25°C. Lipids were solubilized in 500 μL of CDCl_3 , 200 μL methanol, and 50 μL
706 aqueous EDTA solution (200 mM at pH 6), **E: structure of polymyxin B.**
707



709 **Figure S4:** Experimental (black) and simulated spectra (red) of *vibrio splendidus* model
710 membranes without marennine and in the presence of 200 $\mu\text{g}/\text{mL}$ marennine at 25 and 50 °C. The
711 ellipsoid long-to-short axis ratio ρ is indicated.

712